

Temporal Exposure Dependence Bias in Vaccine Efficacy Trials

Hiroyasu Ando[†]

Department of Biostatistics, University of California, Los Angeles, California, 90095, USA.

A. James O'Malley

Department of Biomedical Data Science, Geisel School of Medicine at Dartmouth, Lebanon, NH 03756, USA.

The Dartmouth Institute for Health Policy and Clinical Practice, Geisel School of Medicine at Dartmouth, Lebanon, NH 03756, USA.

Akihiro Nishi[‡]

Department of Epidemiology, University of California, Los Angeles, California, 90095, USA.

Summary. Using time-to-event methods such as Cox proportional hazards models, it is well established that unmeasured heterogeneity in exposure or infection risk can lead to downward bias in point estimates of the per-contact vaccine efficacy (VE) in infectious disease trials. In this study, we explore an unreported source of bias—arising from temporally correlated exposure status—that is typically unmeasured and overlooked in standard analyses. Although this form of bias can plausibly affect a wide range of VE trials, it has received limited empirical attention. We develop a mathematical framework to characterize the mechanism of this bias and derive a closed-form approximation to quantify its magnitude without requiring direct measurement of exposure. Our findings show that, under realistic parameter settings, the resulting bias can be substantial. These results suggest that temporally correlated exposure should be recognized as a potentially important factor in the design and analysis of infectious disease vaccine trials.

Keywords: Causal Inference; Cox Hazard Models; Vaccine Efficacy; Clinical Trials; Infectious Diseases; Exposure Status

1. Introduction

Using a time-weighted hazard ratio analysis, such as the Cox hazard models, it is well established that unmeasured heterogeneity in exposure or infection risk can induce down-

[†]*Address for correspondence:* Hiroyasu Ando, Department of Biostatistics, University of California, Los Angeles, California, 90095, USA. Email: hiro1999@ucla.edu

[‡]*Address for correspondence:* Akihiro Nishi, Department of Epidemiology, University of California, Los Angeles, California, 90095, USA. Email: akihironishi@ucla.edu

ward bias in point estimates of the per-contact vaccine efficacy (VE) in infectious disease trials (Kahn et al., 2018; O'Hagan et al., 2014). In this context, we define the per-contact VE as the proportional reduction, attributable to vaccination, in the probability that a single exposure results in infection (O'Hagan et al., 2014; Lipsitch et al., 2022). A previously proposed directed acyclic graph (DAG) for VE trials illustrates how unmeasured heterogeneity can induce a spurious association between vaccination status and infection status over time (O'Hagan et al., 2014).

For example, O'Hagan et al. (2014) made an example in which $\mathbf{A} \in \{0, 1\}$ is a potential vaccine and $\mathbf{Y}_t \in \{0, 1\}$ is a chlamydia infection at time t (see Fig. 1). Let \mathbf{E}_t be the number of exposures to the infection experienced at time t . Being a sex worker, $\mathbf{U} \in \{0, 1\}$, is not measured but known to increase the risk of bacterial vaginosis and, thus, is another risk factor for a chlamydia infection (heterogeneity in infection risk). Because study participants leave the cohort when infected, for example, at time $t - 1$, \mathbf{U} makes a “backdoor path,” opened by $\mathbf{A} \rightarrow \boxed{\mathbf{Y}_{t-1}} \leftarrow \mathbf{U} \rightarrow \mathbf{Y}_t$, which produces a spurious association between \mathbf{A} and \mathbf{Y}_t in addition to the causal path of $\mathbf{A} \rightarrow \mathbf{Y}_t$.

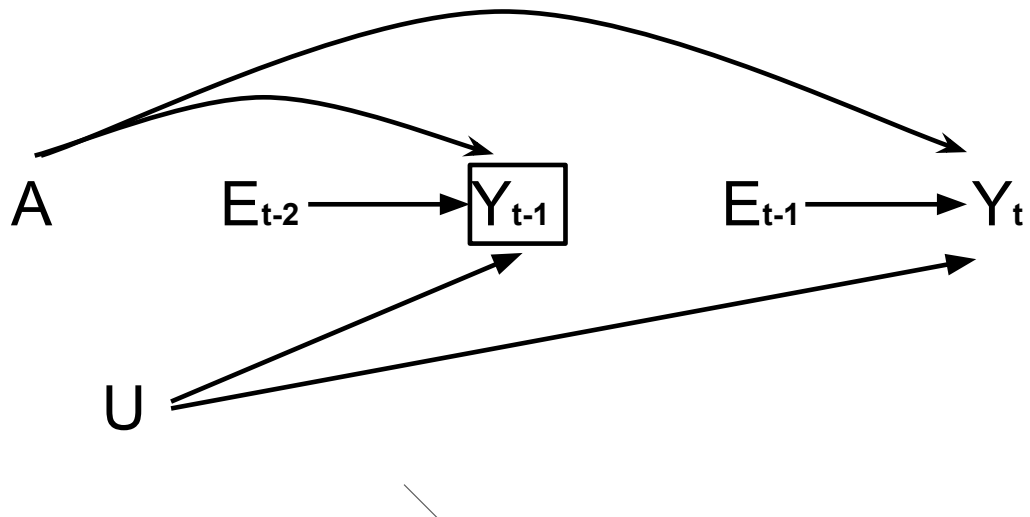


Fig. 1. Causal diagram for a double-blind randomized trial with $\mathbf{A} \rightarrow \boxed{\mathbf{Y}_{t-1}} \leftarrow \mathbf{U} \rightarrow \mathbf{Y}_t$

Kahn et al. (2018) created an example in which vaccine trial participants are drawn from multiple communities, in which the number of imported cases (\mathbf{U}) varied upon the beginning of their network-based simulations (see Fig. 2). Such initial heterogeneity produces variation between communities in the level of the local epidemic over the follow-up period, resulting in a backdoor path, opened by $\mathbf{A} \rightarrow \boxed{\mathbf{Y}_{t-1}} \leftarrow \mathbf{E}_{t-2} \leftarrow \mathbf{U} \rightarrow \mathbf{E}_{t-1} \rightarrow \mathbf{Y}_t$. Please note that the initial heterogeneity (\mathbf{U}) is given regardless of \mathbf{A} . Thus, all participants (vaccinated or unvaccinated) are exchangeable at the beginning of the VE trial.

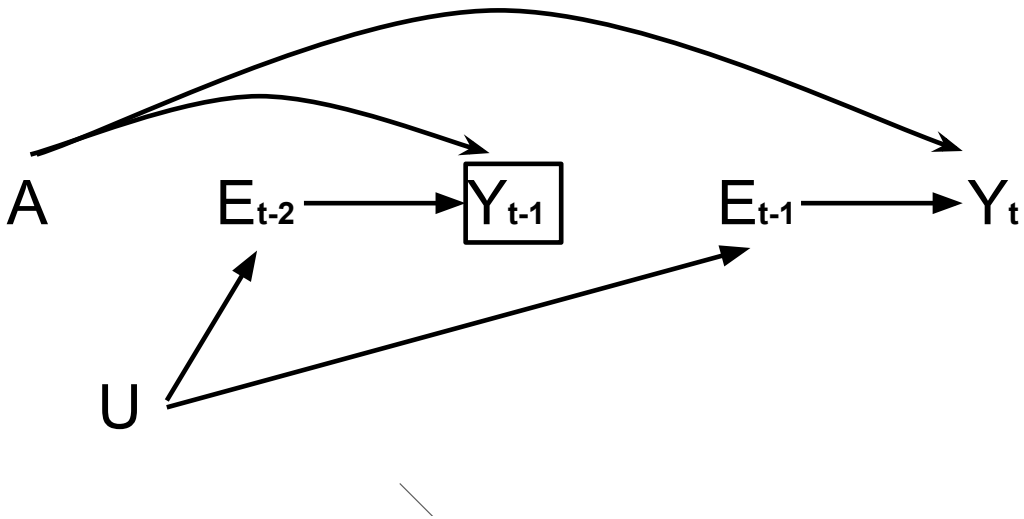


Fig. 2. Causal diagram for a double-blind randomized trial with $A \rightarrow \boxed{Y_{t-1}} \leftarrow E_{t-2} \leftarrow U \rightarrow E_{t-1} \rightarrow Y_t$

To block the backdoor paths described in Fig. 1 and 2, it is vital to proactively obtain and measure all potential variables causing the heterogeneity in the exposure or infection risk. As long as these variables are incorporated in the model (e.g., using a stratified Cox model), the backdoor path producing the spurious association between A and Y_t is blocked, and the bias would be mitigated. This bias is a pitfall since it could happen even in randomized controlled trials (RCTs), which are considered the gold standard for eliminating bias from unmeasured confounding factors (O'Hagan et al., 2014; Halloran et al., 1996).

Here, we discuss a different possibility of bias produced by a direct path from exposure status at time $t - 2$ (E_{t-2}) to that at time $t - 1$ (E_{t-1}) without the existence of U (see Fig. 3). Although the arrow between E_{t-2} and E_{t-1} has been rarely drawn in the DAGs of infectious VE trials in prior literature (Kahn et al., 2018; O'Hagan et al., 2014; Stensrud and Smith, 2023), we claim that it occurs on most occasions.

When $E_{t-2} = 1$ (exposed), the infectious individuals are the most likely to be infectious at time $t - 1$ and keep the focal individual exposed. The infectious period of the infectious individual is often not one time unit (day) but multiple days (e.g., three days on average in the early stage of the COVID-19 pandemic (He et al., 2020)). As long as the focal participant and the infectious individual keep engaging in similar daily interactions at workplaces, schools, and other locations, the exposure will happen again at time $t - 1$ ($E_{t-1} = 1$). This scenario produces a "backdoor path", $A \rightarrow \boxed{Y_{t-1}} \leftarrow E_{t-2} \rightarrow E_{t-1} \rightarrow Y_t$ (Fig. 3). Notably, in a special case where exposure status remains constant across time (i.e.,

$E_{t-j} = E_{t-h}$ for all j, h), earlier exposures such as E_{t-2} may have a direct influence on the outcome Y_t , bypassing intermediate steps.

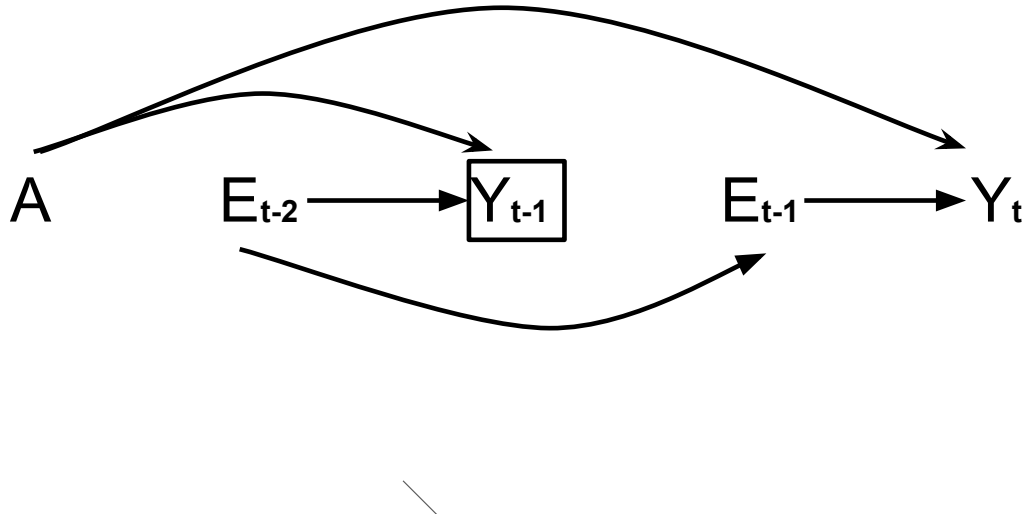


Fig. 3. Causal diagram for a double-blind randomized trial with $A \rightarrow [Y_{t-1}] \leftarrow E_{t-2} \rightarrow E_{t-1} \rightarrow Y_t$

Because the exposure variables (E_{t-2} and E_{t-1}) are typically difficult to measure and therefore unavailable in most datasets, the per-contact VE is often estimated using a time-weighted hazard ratio analysis, which is enabled by the Cox proportional hazard models. Otherwise, following Halloran et al. (2010), the per-contact VE can be estimated as:

$$\widehat{VE}_{S,SAR} = 1 - \frac{\# \text{ vaccinated infections}/\# \text{ vaccinated contacts}}{\# \text{ unvaccinated infections}/\# \text{ unvaccinated contacts}} \quad (1)$$

This expression captures the relative risk of infection given exposure, comparing vaccinated and unvaccinated individuals.

Such bias could plausibly arise in any infectious disease VE trials, yet empirical demonstrations of this phenomenon remain scarce. In this article, we aim to disentangle the mechanism underlying this bias and to quantify its magnitude without relying on direct exposure information.

This paper is organized as follows. Section 2 outlines the modeling framework used in our study. Sections 3 and 4 derive an approximation method to quantify the magnitude of the bias. In Section 5, we evaluate the accuracy of this approximation through simulation studies, examine the behavior of the bias under various scenarios, and apply the proposed methodology to the ChAdOx1 nCoV-2019 (Oxford–AstraZeneca) COVID-19 vaccine trial.

2. Modeling Structure

In this section, we outline the underlying mechanism of the proposed bias and present a modeling framework to facilitate its identification.

2.1. Bias Mechanism

We define \widehat{v}^* as the estimator for VE from the Cox proportional hazards model (Cox, 1972):

$$\widehat{v}^* = 1 - \frac{h(t \mid \mathbf{A} = 1; \hat{\theta})}{h(t \mid \mathbf{A} = 0; \hat{\theta})} = 1 - \exp(\hat{\theta}), \quad (2)$$

where $\mathbf{A} \in \{0, 1\}$ is a potential vaccine, and $\hat{\theta}$ is the maximum likelihood estimator (MLE) of the treatment effect. The function $h(t \mid \mathbf{A}; \hat{\theta})$ denotes the estimated hazard at time t , conditional on treatment assignment \mathbf{A} . Importantly, this hazard function is not conditioned on the number of exposures.

The parameter $\hat{\theta}$ is obtained by maximizing the partial likelihood function:

$$L(\theta) = \prod_{j=1}^D \frac{h(t \mid \mathbf{A}_j = 1; \theta)}{\sum_{i \in R_j} h(t \mid \mathbf{A}_i = 1; \theta)} = \prod_{j=1}^D \frac{\exp(\mathbf{A}_j \cdot \theta)}{\sum_{i \in R_j} \exp(\mathbf{A}_i \cdot \theta)}, \quad (3)$$

where R_j is the risk set at event time j , which includes both exposed and unexposed individuals. We hypothesize that this estimator, \widehat{v}^* is biased due to the strong association between \mathbf{E}_{t-2} and \mathbf{E}_{t-1} , which reflects temporal dependence in exposure risk. The resulting bias arises from differences in the number of exposures between the vaccinated and placebo groups.

In infectious disease contexts, individuals may be exposed to infection over multiple time points following contact with infectious peers. Vaccinated individuals are more likely to experience exposure events than those in the placebo group. This occurs because vaccination reduces the risk of infection, allowing vaccinated individuals to remain susceptible and at risk of exposure for a longer duration from the same infectious peers. In contrast, individuals in the placebo group are more likely to become infected earlier, thus experiencing fewer exposure events from those same peers.

As a result, the number of exposures between the vaccinated and placebo groups differs. Based on the equations (2) and (3), the estimated hazard function does not reflect on the number of exposures of each individual, thus \widehat{v}^* does not account for the exposure imbalance, leading to a downward bias.

2.2. Infectious Window Model

In the following, we introduce several assumptions to model the difference in the number of exposures between the vaccinated and placebo groups.

2.2.0.1. *Assumption 1 (Baseline Sampling).* A large random sample is drawn at time $t = 1$ and is followed over time. Note that at baseline, individuals are randomly assigned to either the vaccine group ($\mathbf{A} = 1$) or the placebo group ($\mathbf{A} = 0$).

2.2.0.2. *Assumption 2 (Infectious Window).* An infectious window refers to a temporary compartment that an individual enters. Once entered (e.g., at time t), the individual remains exposed for a few time points following some random variable, $\mathbf{I} > 0$, which takes values in $\mathbb{N}_{>0}$.

2.2.0.3. *Assumption 3 (Rare and Uniform Entry).* Each individual has a small probability m of entering into an infectious window on any given day. For example, $m < 0.01$. This probability is constant across time and assumed to be independent and identically distributed (i.i.d.) across all individuals in the sample.

2.2.0.4. *Assumption 4 (Per-Contact Transmissibility).* During each time point within an infectious window, the individual is exposed to a pathogen and faces a probability $p \in (0, 1)$ of becoming infected. These temporal infection events are assumed to be independent and identically distributed (i.i.d.) across time points in the window.

2.2.0.5. *Assumption 5 (Vaccine Efficacy).* Per-contact *VE* is defined as the proportional reduction, attributable to vaccination in the probability that a single exposure results in infection. For example, when vaccinated the per-contact transmissibility is $p \cdot (1 - v)$ for $v \in (0, 1)$.

2.2.0.6. *Assumption 6 (One-time Infection).* Once infected, an individual exits the risk pool permanently and can no longer enter into an infectious window. That is, reinfection does not occur within the study period.

3. Quantifying Bias Magnitude

In the discrete-time Cox proportional hazards model for survival data, the hazard at time t conditional on covariates \mathbf{A} is defined as:

$$h^*(t \mid \mathbf{A}; \theta) = \mathbb{P}_\theta(\mathbf{Y}_{t+1} = 1 \mid \mathbf{Y}_t = 0, \mathbf{A}), \quad (4)$$

where $\mathbf{A} \in \{0, 1\}$ is a potential vaccine and $\mathbf{Y}_t \in \{0, 1\}$ represents the infection status at time t . We assume each individual may be infected only once during the study period.

Let \mathbf{E}_t be a latent variable representing the number of exposures at time t . The hazard can then be decomposed using the law of total probability:

$$\mathbb{P}_\theta(\mathbf{Y}_{t+1} = 1 \mid \mathbf{Y}_t = 0, \mathbf{A}) = \sum_{e=1}^{\infty} \mathbb{P}_\theta(\mathbf{Y}_{t+1} = 1 \mid \mathbf{Y}_t = 0, \mathbf{A}, \mathbf{E}_t = e) \cdot \mathbb{P}_\theta(\mathbf{E}_t = e \mid \mathbf{Y}_t = 0, \mathbf{A}). \quad (5)$$

Assuming that multiple exposures are rare (i.e., $m \approx 0$ where m is probability of entering into an infectious window), we approximate the sum by the $e = 1$ term:

$$\mathbb{P}_\theta(\mathbf{Y}_{t+1} = 1 \mid \mathbf{Y}_t = 0, \mathbf{A}) \approx \mathbb{P}_\theta(\mathbf{Y}_{t+1} = 1 \mid \mathbf{Y}_t = 0, \mathbf{A}, \mathbf{E}_t = 1) \cdot \mathbb{P}_\theta(\mathbf{E}_t = 1 \mid \mathbf{Y}_t = 0, \mathbf{A}), \quad (6)$$

Defining the per-contact hazard as

$$h(t \mid \mathbf{A}; \theta) := \mathbb{P}_\theta(\mathbf{Y}_{t+1} = 1 \mid \mathbf{Y}_t = 0, \mathbf{A}, \mathbf{E}_t = 1), \quad (7)$$

we obtain the approximation:

$$h^*(t \mid \mathbf{A}; \theta) \approx h(t \mid \mathbf{A}; \theta) \cdot \mathbb{P}_\theta(\mathbf{E}_t = 1 \mid \mathbf{Y}_t = 0, \mathbf{A}). \quad (8)$$

Next, defining the VE based on the discrete-time Cox proportional hazards model as:

$$v^* = 1 - \frac{h^*(t \mid \mathbf{A} = 1; \theta)}{h^*(t \mid \mathbf{A} = 0; \theta)}, \quad (9)$$

then substituting the hazard decomposition yields:

$$\begin{aligned} v^* &\approx 1 - \frac{h(t \mid \mathbf{A} = 1; \theta) \cdot \mathbb{P}_\theta(\mathbf{E}_t = 1 \mid \mathbf{Y}_t = 0, \mathbf{A} = 1)}{h(t \mid \mathbf{A} = 0; \theta) \cdot \mathbb{P}_\theta(\mathbf{E}_t = 1 \mid \mathbf{Y}_t = 0, \mathbf{A} = 0)} \\ &= 1 - (1 - v) \cdot \frac{\mathbb{P}_\theta(\mathbf{E}_t = 1 \mid \mathbf{Y}_t = 0, \mathbf{A} = 1)}{\mathbb{P}_\theta(\mathbf{E}_t = 1 \mid \mathbf{Y}_t = 0, \mathbf{A} = 0)}, \end{aligned} \quad (10)$$

where

$$v = 1 - \frac{h(t \mid \mathbf{A} = 1; \theta)}{h(t \mid \mathbf{A} = 0; \theta)} \quad (11)$$

is the per-contact VE.

This result highlights that the VE based on the discrete-time Cox proportional hazards model, v^* , may be deviated from the per-contact VE due to differential exposure risks between vaccine and placebo groups.

The key quantity influencing the bias is the relative exposure probability:

$$\frac{\mathbb{P}_\theta(\mathbf{E}_t = 1 \mid \mathbf{Y}_t = 0, \mathbf{A} = 1)}{\mathbb{P}_\theta(\mathbf{E}_t = 1 \mid \mathbf{Y}_t = 0, \mathbf{A} = 0)}. \quad (12)$$

Adjusting for this term is essential to recover the per-contact VE.

4. Relative Exposure Probability

We consider the probability that an individual enters an infectious window at time t , given that they are uninfected up to time t and assigned to the placebo group:

$$\mathbb{P}_\theta(\mathbf{E}_t = 1 \mid \mathbf{Y}_t = 0, \mathbf{A} = 0).$$

Let $\mathbf{X} = (X_1, \dots, X_t) \in \{0, 1\}^t$ denote the binary vector representing whether an individual enters an infectious window at each time point from 1 to t . Then the above probability can be written as:

$$\mathbb{P}_\theta(\mathbf{E}_t = 1 \mid \mathbf{Y}_t = 0, \mathbf{A} = 0) = \sum_{\mathbf{x} \in \{0,1\}^t} \mathbb{P}_\theta(\mathbf{E}_t = 1, \mathbf{X} = \mathbf{x} \mid \mathbf{Y}_t = 0, \mathbf{A} = 0).$$

Under the rare entry assumption $m \approx 0$, the probability of entering multiple infectious windows is negligible. Therefore, we restrict the summation to the set

$$\mathcal{W} = \{\mathbf{w} \in \{0, 1\}^t : \|\mathbf{w}\|_1 = 1\},$$

and approximate:

$$\begin{aligned} \mathbb{P}_\theta(\mathbf{E}_t = 1 \mid \mathbf{Y}_t = 0, \mathbf{A} = 0) &\approx \sum_{\mathbf{w} \in \mathcal{W}} \mathbb{P}_\theta(\mathbf{E}_t = 1, \mathbf{X} = \mathbf{w} \mid \mathbf{Y}_t = 0, \mathbf{A} = 0) \\ &= \frac{1}{\mathbb{P}_\theta(\mathbf{Y}_t = 0, \mathbf{A} = 0)} \sum_{\mathbf{w} \in \mathcal{W}} \mathbb{P}_\theta(\mathbf{E}_t = 1, \mathbf{X} = \mathbf{w}, \mathbf{Y}_t = 0, \mathbf{A} = 0) \\ &= \frac{m \cdot (1-m)^{t-1}}{1 - O(m \cdot p)} \sum_{s=0}^t (1-p)^s \cdot \mathbb{P}(\mathbf{I} > s), \end{aligned} \quad (13)$$

where $\mathbb{P}(\mathbf{I} > s)$ is the probability that the infectious window, once entered at time s , includes time t . $O(m \cdot p)$ denotes the approximate probability of having been infected by time t .

For the vaccinated group, where the per-contact transmissibility is reduced to $p \cdot (1-v)$, we similarly have:

$$\mathbb{P}_\theta(\mathbf{E}_t = 1 \mid \mathbf{Y}_t = 0, \mathbf{A} = 1) \approx \frac{m \cdot (1-m)^{t-1}}{1 - O(m \cdot p \cdot (1-v))} \sum_{s=0}^t \{1 - p(1-v)\}^s \cdot \mathbb{P}(\mathbf{I} > s).$$

Given $m \approx 0$, taking the ratio of the exposure probabilities yields:

$$\frac{\mathbb{P}_\theta(\mathbf{E}_t = 1 \mid \mathbf{Y}_t = 0, \mathbf{A} = 1)}{\mathbb{P}_\theta(\mathbf{E}_t = 1 \mid \mathbf{Y}_t = 0, \mathbf{A} = 0)} \approx \frac{\sum_{s=0}^t (1 - p \cdot (1-v))^s \cdot \mathbb{P}(\mathbf{I} > s)}{\sum_{s=0}^t (1-p)^s \cdot \mathbb{P}(\mathbf{I} > s)}. \quad (14)$$

Here, the numerator accounts for a reduced per-contact transmissibility in the vaccine group, denoted as $p \cdot (1-v)$.

To simplify computation, we propose a truncated approximation using a small integer $R > 0$ (e.g., $1 \leq R \leq 10$), yielding:

$$\frac{\mathbb{P}_\theta(\mathbf{E}_t = 1 \mid \mathbf{Y}_t = 0, \mathbf{A} = 1)}{\mathbb{P}_\theta(\mathbf{E}_t = 1 \mid \mathbf{Y}_t = 0, \mathbf{A} = 0)} \approx \frac{\sum_{s=0}^R \mathbb{P}(\mathbf{I} > s) \cdot \{1 - p \cdot (1-v)\}^s}{\sum_{s=0}^R \mathbb{P}(\mathbf{I} > s) \cdot (1-p)^s}. \quad (15)$$

This approximation facilitates practical evaluation of the relative exposure probability under a finite time horizon, while preserving the essential dynamics of prolonged infectious windows and differential per-contact transmissibility due to vaccination.

With this approximation method, the uniform entry assumption can be relaxed. Specifically, the probability of entering an infectious window, m , can be assumed constant only over the truncated horizon of length R . This allows for longer-term fluctuations in m , thereby capturing more realistic infectious dynamics over the full study period.

5. Result

5.1. Simulation Study

We conducted simulation studies based on the infectious window model (see Section 2.2) to evaluate the validity of equations (10) and (15).

In this setup, individuals were allowed to enter an infectious window at each time point with a small probability $m \approx 0$. We fixed this entry probability at $m = 0.01$. The duration of each infectious window was modeled by a random variable $\mathbf{I} \sim \text{Geometric}(1/3)$. Importantly, individuals could enter multiple infectious windows over time.

During each infectious window, an individual faced a probability of infection $p \in (0, 1)$ at each time point. We considered three values for the per-contact transmissibility: $p \in \{0.05, 0.1, 0.15\}$. Once an individual became infected, they were no longer eligible to enter future infectious windows, thereby preventing subsequent reinfection.

We assumed that vaccination reduces the per-contact transmissibility by a factor of $0 < v < 1$, such that the per-contact transmissibility for vaccinated individuals becomes $p \cdot (1 - v)$. We evaluated performance under three efficacy levels: $v \in \{0.3, 0.6, 0.9\}$.

A total of 10,000 individuals were simulated, with equal randomization into vaccine and placebo groups (5,000 each) at baseline. The trial was simulated over 180 time units, interpreted as days.

At the end of the trial (day 180), we compared the Cox-based VE estimator, \widehat{v}^* , with the per-contact VE estimator, \widehat{v} , derived by solving equation (16) that incorporates the per-contact transmissibility p , the distribution of the infectious window duration \mathbf{I} , and \widehat{v}^* ,

$$\widehat{v}^* = 1 - (1 - \widehat{v}) \cdot \frac{\mathbb{P}_\theta(\mathbf{E}_t = 1 \mid \mathbf{Y}_t = 0, \mathbf{A} = 1)}{\mathbb{P}_\theta(\mathbf{E}_t = 1 \mid \mathbf{Y}_t = 0, \mathbf{A} = 0)}. \quad (16)$$

Following equation (15), the conditional probability was approximated, assuming $R = 10$ as:

$$\frac{\mathbb{P}_\theta(\mathbf{E}_t = 1 \mid \mathbf{Y}_t = 0, \mathbf{A} = 1)}{\mathbb{P}_\theta(\mathbf{E}_t = 1 \mid \mathbf{Y}_t = 0, \mathbf{A} = 0)} \approx \frac{\sum_{s=0}^{10} \mathbb{P}(\mathbf{I} > s) \cdot \{1 - p \cdot (1 - \widehat{v})\}^s}{\sum_{s=0}^{10} \mathbb{P}(\mathbf{I} > s) \cdot (1 - p)^s}. \quad (17)$$

This derivation was theoretically justified by the delta method. Letting $\beta = \log(1 - v^*)$, we applied the asymptotic result:

$$\sqrt{n}(\hat{\beta} - \beta) \xrightarrow{d} \mathcal{N}(0, \sigma^2) \Rightarrow \sqrt{n}(\hat{v} - v) \xrightarrow{d} \mathcal{N}(0, \sigma_v^2), \quad (18)$$

where the delta method was applied to the transformation $g(\beta, I, p) = v$.

Fig. 4, 5, and 6 present the simulation results. In each panel, the red horizontal line represents the per-contact *VE*. These results illustrate that the Cox-based *VE* estimator, \hat{v}^* , exhibits bias with respect to the per-contact *VE*. In contrast, the estimator, \hat{v} , derived from equation (16), consistently reduces this bias across a wide range of parameter settings.

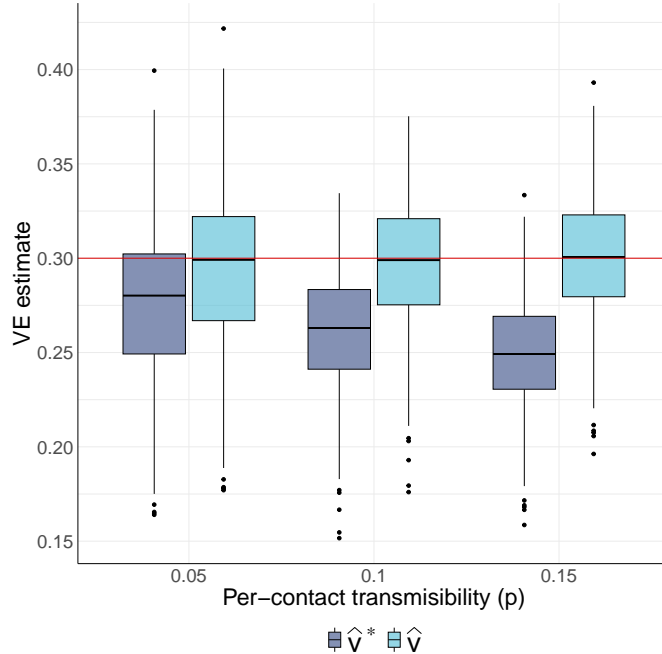


Fig. 4. *VE* estimates over the 500 simulations when $v = 0.3$

5.2. Behavior of Bias

We next examined the behavior of the magnitude of this bias as a function of v , p , and \mathbf{I} . Unlike the simulation analysis, this investigation relied solely on the analytical expression given in equations (10) and (15) with $R = 10$:

$$v^* = 1 - (1 - v) \cdot \frac{\sum_{s=0}^{10} \mathbb{P}(\mathbf{I} > s) \cdot \{1 - p \cdot (1 - v)\}^s}{\sum_{s=0}^{10} \mathbb{P}(\mathbf{I} > s) \cdot (1 - p)^s}. \quad (19)$$

Fig. 7 depicts the relationship between $v \in (0.05, 0.95)$ and the ratio v^*/v , based on equation (19), for three values of per-contact transmissibility: $p \in \{0.05, 0.1, 0.15\}$. As

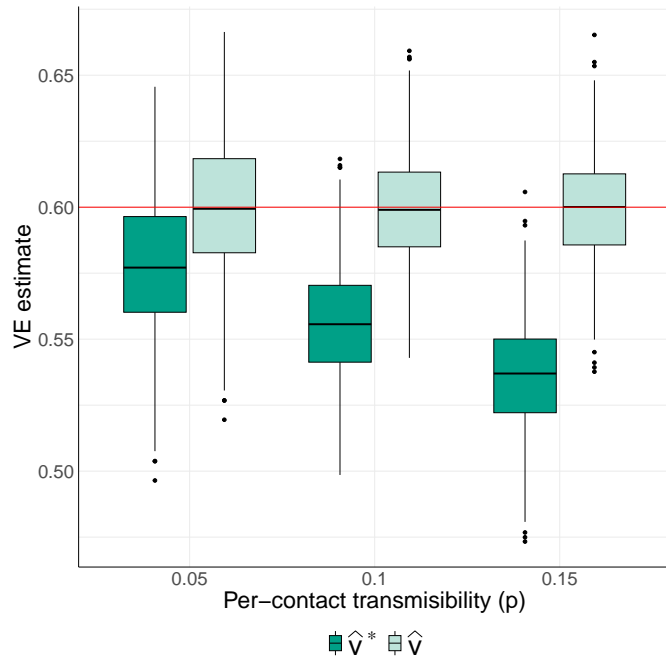


Fig. 5. VE estimates over the 500 simulations when $v = 0.6$

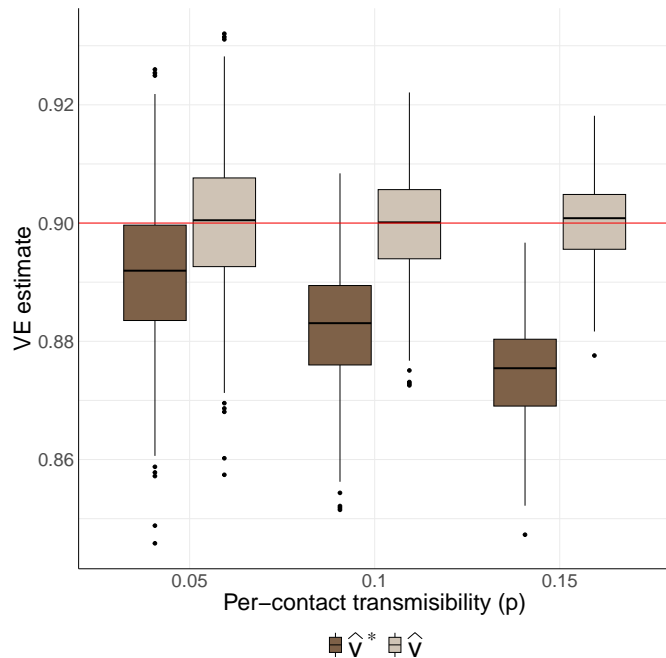


Fig. 6. VE estimates over the 500 simulations when $v = 0.9$

in the simulation setting, the duration of each infectious window was modeled as $\mathbf{I} \sim \text{Geometric}(1/3)$.

Fig. 7 illustrates the proportional relationship between v (the per-contact VE) and v^* (the Cox-based VE). For example, when $v = 0.45$ and $p = 0.05$, the ratio v^*/v is approximately 0.95, indicating a modest underestimation of the per-contact VE by the Cox-based VE estimator, \widehat{v}^* .

As shown in Fig. 7, the deviation between v^* and v increases as v decreases. This suggests that the Cox-based estimator, \widehat{v}^* , becomes proportionally more biased when the per-contact VE is lower. Furthermore, the extent of this deviation is amplified for larger values of p . This means that when the per-contact transmissibility p is high, the Cox-based estimator, \widehat{v}^* , increasingly underestimates the per-contact VE.

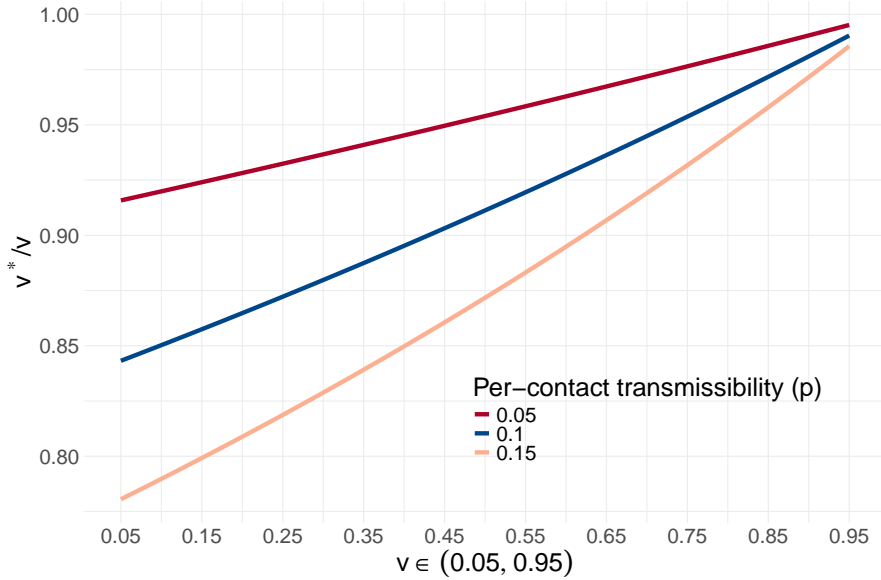


Fig. 7. Relationship between the per-contact VE and the Cox-based VE

5.3. Real Data Example

In this section, we construct the per-contact VE estimators \widehat{v} and its 95% confidence intervals (CIs) using the Cox-based estimator v^* , derived from the ChAdOx1 nCoV-2019 (Oxford–AstraZeneca) COVID-19 vaccine trial, as reported by Falsey et al. (2021).

We focus on the Hispanic or Latinx subgroup, for which the Cox-based VE estimator was reported as $\widehat{v}^* = 0.575$ with a 95% CI of (0.282, 0.748). Notably, the lower bound of this CI falls below the U.S. FDA's minimum Emergency Use Authorization (EUA) threshold of 0.3 (U.S. Food and Drug Administration, 2021).

To obtain the per-contact VE estimator \widehat{v} , we solve equations (16) and (17) with $R = 10$, incorporating the per-contact transmission probability p , the distribution of the infectious window duration \mathbf{I} , and the Cox-based estimator \widehat{v}^* .

Table 1. Per-contact VE estimator, \widehat{v}^* , and their 95% CIs for the Hispanic/Latinx subgroup

| Per-contact Transmissibility | Per-contact VE Estimator (%) | 95% Confidence Interval |
|------------------------------|------------------------------|-------------------------|
| Cox-based (original) | 57.5 | (28.2, 74.8) |
| 0.05 | 59.7 | (30.1, 76.5) |
| 0.1 | 61.8 | (31.9, 78.0) |
| 0.15 | 63.6 | (33.7, 79.3) |

To construct the 95% CI for the per-contact VE , we invert the Wald test. The hypothesis test is formulated as:

$$H_0 : v = v_0 \quad (20)$$

Following equations (10) and (15), and fixing $R = 10$, we define the null-implied Cox-based VE , v_0^* , as:

$$v_0^* \approx 1 - (1 - v_0) \cdot \frac{\sum_{s=0}^{10} \mathbb{P}(I > s) \cdot \{1 - p \cdot (1 - v_0)\}^s}{\sum_{s=0}^{10} \mathbb{P}(I > s) \cdot (1 - p)^s} \quad (21)$$

Under H_0 , the corresponding log hazard ratio is:

$$\beta_0 = \log(1 - v_0^*) \quad (22)$$

The Wald test statistic is given by:

$$Z = \frac{\widehat{\beta} - \beta_0}{\text{SE}(\widehat{\beta})} \sim \mathcal{N}(0, 1) \quad (23)$$

where $\widehat{\beta}$ is the maximum partial likelihood estimate of the log hazard ratio, and $\text{SE}(\widehat{\beta})$ is its standard error.

To construct the 95% CI for the per-contact VE , we identify values of v_0 satisfying:

$$\left| \frac{\widehat{\beta} - \beta_0}{\text{SE}(\widehat{\beta})} \right| < z_{0.975} \quad (24)$$

with $z_{0.975} \approx 1.96$, the 97.5th percentile of the standard normal distribution.

Following prior studies (Nishi et al., 2020; He et al., 2020), we modeled the infectious window \mathbf{I} as Geometric(1/3) and consider three plausible values for the per-contact transmissibility: $p \in \{0.05, 0.1, 0.15\}$.

The resulting per-contact VE estimators, \widehat{v} , and their 95% CIs are presented in Table 1. These results suggest that the originally reported Cox-based estimator, \widehat{v}^* , may underestimate the per-contact VE . Importantly, across all considered values of p , the lower bounds of the derived CIs are 30.1%, 31.9%, and 33.7%, respectively—all of which exceed the FDA’s minimum EUA threshold of 30% (U.S. Food and Drug Administration, 2021).

6. Discussion

We demonstrate a new potential source of bias in VE trials due to the strong association of \mathbf{E}_{t-2} and \mathbf{E}_{t-1} . As long as there is a disproportionate number of exposures between the vaccine and placebo groups during the trial period, VE estimators not conditioned on knowledge of exposure to infection, such as those from the Cox proportional hazards model, will be biased in terms of the per-contact VE . Since information on exposure is usually unavailable and, thus, not used in data analysis, the bias mentioned above might occur in any infectious disease VE trials, and they might underestimate the per-contact VE .

Although the magnitude of this bias is typically small and unlikely to produce the severely misleading per-contact VE estimators in most scenarios, its presence should not be overlooked. Notably, under realistic epidemiological conditions—such as the per-contact transmissibility of $p = 0.15$, the infectious window of $\mathbf{I} \sim \text{Geometric}(1/3)$, and the per-contact VE of 0.75—the difference between the per-contact VE and the Cox-based VE reaches more than 7.5% (see Fig. 7). This level of distortion is not trivial in the context of clinical trial evaluation and regulatory decision-making. Therefore, this potential bias should be acknowledged as a potentially relevant factor in the design and analysis of VE trials for infectious diseases. Its extent should be quantitatively assessed and, where appropriate, mitigated through design adaptations or statistical adjustments in order to ensure accurate and robust inference.

In this paper, we presented a plausible statistical adjustment framework to enable the estimation of the per-contact VE and its associated 95% confidence intervals (CIs). However, this approach relies critically on the appropriate specification of the infectious window distribution, \mathbf{I} and the per-contact transmissibility probability, p , both of which are subject to strong assumptions (see Section 2.2).

Careful selection of these parameters is essential—not only for ensuring statistical validity, but also for maintaining scientific rigor and ethical responsibility in the interpretation and dissemination of VE estimates. Given the sensitivity of the results to these assumptions, we recommend that the per-contact VE estimators and their 95% CIs derived under this method be interpreted with caution. At a minimum, they should be evaluated under a range of plausible values for p and \mathbf{I} , and their role should be considered supplementary when making inferential or policy-relevant claims regarding VE .

Future research should focus on developing methods for estimating the distribution of \mathbf{I} and per-contact transmissibility, and on incorporating these components directly into the likelihood framework. Such methodological advances would enable more accurate and less assumption-dependent inference in VE studies for infectious diseases.

7. Disclosure Statement

AN is a consultant to Vacan, Inc. and obtained an honorarium from Taisho Pharmaceutical Co., Ltd., which had no role in the project.

8. Data and Software Availability

All analysis was done in the R environment (R version 4.3.2). The code and available data to reconstruct the analyses of this paper are available at <https://github.com/Ankoudon/>.

9. Acknowledgements

This article is based upon work supported by the National Institutes of Health (K01AI166347), the National Science Foundation (NSF#2230125), the Japan Science and Technology Agency (JPMJPR21R8), and the National Institutes of Health (P01AG019783, P20GM148278). The content is solely the responsibility of the authors and does not necessarily represent the official views of the funders.

10. Author Contributions

HA discovered the bias. HA derived the formulas and methodologies, which were validated by AJO. HA, AN, and AJO wrote the manuscript. AN contributed laboratory resources.

References

Cox, D. R. (1972). Regression models and life-tables. *Journal of the Royal Statistical Society Series B* 34(2), 187–220.

Falsey, A., M. Sobieszczyk, I. Hirsch, and et al. (2021). Phase 3 safety and efficacy of azd1222 (chadox1 ncov-19) covid-19 vaccine. *The New England Journal of Medicine* 385(25), 2348–2360.

Halloran, M., I. Longini, and C. Struchiner (1996). Estimability and interpretation of vaccine efficacy using frailty mixing models. *American Journal of Epidemiology* 144(1), 83–97.

Halloran, M., I. Longini, and C. Struchiner (2010). *Design and Analysis of Vaccine Studies*.

He, X., E. Laum, P. Wu, and et al. (2020). Temporal dynamics in viral shedding and transmissibility of covid-19. *Nature Medicine* 26(5), 672–675.

Kahn, R., M. Hitchings, S. Bellan, and et al. (2018). Impact of stochastically generated heterogeneity in hazard rates on individually randomized vaccine efficacy trials. *Clinical Trials* 15(2), 207–211.

Lipsitch, M., F. Krammer, G. Regev-Yochay, and et al. (2022). Sars-cov-2 breakthrough infections in vaccinated individuals: measurement, causes and impact. *Nature Reviews Immunology* 22(1), 57–65.

Nishi, A., G. Dewey, A. Endo, and et al. (2020). Network interventions for managing the covid-19 pandemic and sustaining economy. *Proceedings of the National Academy of Sciences* 117(48), 30285–30294.

O'Hagan, J., M. Lipsitch, and M. Hernan (2014). Estimating the per-exposure effect of infectious disease interventions. *Epidemiology* 25(1), 134–138.

Stensrud, M. and L. Smith (2023). Identification of vaccine effects when exposure status is unknown. *Epidemiology* 34(2), 216–224.

U.S. Food and Drug Administration (2021). Emergency use authorization (eua) for an unapproved product review memorandum.